

for molecules with a single long chain. Both chains are found to be important in the packing. Differences in micelle characteristics for lecithins with the same total carbon atoms in the fatty acyl chains reflect the nonequivalence of the two fatty acyl chains. While the S_N1 and S_N2 chains are not equivalent in packing in the disordered micelle hydrocarbon core,⁷ this difference is found to be less than that in the bilayer structure. Finally, the form factor of these rod-like short-chain lecithin micelles can be approximately taken to be that of a rigid rod even when they grow up to a length of a few thousand angstroms, having a length to diameter ratio larger than 100. This point is inferred from the constant R_c and N/L values found for each lecithin species at all the concentrations studied.

The detailed structures of short-chain lecithin micelles are useful for understanding hydrolysis rates of water-soluble phospholipases. These enzymes show higher specific activities toward micellar lecithins than toward lecithins packed in a bilayer. It has been suggested that this may be due to the larger area per head group, i.e., greater accessibility, of lecithins in micelles ($\approx 100 \text{ \AA}^2$ for dihexanoyl-PC) compared to those in bilayers ($\approx 65 \text{ \AA}^2$). For

short-chain lecithins with 14 or more carbons in the fatty acyl chains, the micelles are long spherocylinders. While head group areas are $90\text{--}95 \text{ \AA}^2$ in the end caps, the majority of the lecithin molecules are in the long rod sections with considerably smaller head group areas ($70\text{--}75 \text{ \AA}^2$). Since phospholipase C from *Bacillus cereus* has essentially the same activity toward all these short-chain lecithins, substrate head group area alone is probably not the major cause of the activity difference between micelles and bilayer packed lecithins.

Acknowledgment. We are grateful to Dr. Benno Schoenborn of the Biology Department of Brookhaven National Laboratory for granting sufficient beam time for the experiment and to Dr. D. K. Schneider for assistance in using the Biology low-angle neutron spectrometer. We would also like to thank Drs. W. C. Koehler, G. D. Wignall, and J. Hayter for help in using the 30-M SANS spectrometer at NCSASR, ORNL. This research is supported by a NSF grant administrated through the Center for Materials Science and Engineering (S.-H.C.) and NIH Grant GM26762 (M.F.R.).

Nuclear Relaxation in the Magnetic Coupled System $\text{Cu}_2\text{Co}_2\text{SOD}$. Histidine-44 Is Detached upon Anion Binding

L. Banci, I. Bertini,* C. Luchinat, and A. Scozzafava

Contribution from the Department of Chemistry, University of Florence, Florence, Italy.
Received June 19, 1986

Abstract: The ^1H NMR spectra of bovine erythrocyte superoxide dismutase in which zinc is substituted by cobalt ($\text{Cu}_2\text{Co}_2\text{SOD}$) have been recorded at 60, 90, 200, and 400 MHz and compared with those already reported at 300 MHz. The experimental T_1 and T_2 values have been related to the experimental (from X-ray) metal proton distances, thus obtaining a detailed assignment of the signals and the electronic relaxation times (τ_s) of the two metal ions in the coupled system. This has required some critical considerations on the available theory since no such approach had been attempted before on a magnetically coupled system. Comparison of $\text{Cu}_2\text{Co}_2\text{SOD}$ with $\text{Cu}_2\text{Zn}_2\text{SOD}$, on the one hand, and with $\text{E}_2\text{Co}_2\text{SOD}$ (E = empty), on the other, has shown that in the coupled system τ_s of copper is decreased by two orders of magnitude and that of cobalt by a factor of 3. The ^1H NMR spectra at 300 MHz for the N_3^- derivative have been reanalyzed and the T_1 values have been measured. It is shown that His-44 is the one which undergoes detachment upon anions binding, since the isotropic shifts of its protons vanish. However, some paramagnetic effect is measured on T_1 which allowed us to envisage the new position of His-44 within the protein.

Bovine erythrocyte superoxide dismutase is a dimeric protein of MW 32 000, with each subunit containing a catalytically essential copper ion bridged by an histidinato residue to a solvent inaccessible zinc ion ($\text{Cu}_2\text{Zn}_2\text{SOD}$). Figure 1 schematically shows the spatial arrangement of the resulting dimetallic cluster as it appears from the 2- \AA resolution X-ray structure.¹ It has been shown that zinc(II) can be replaced by cobalt(II)²⁻⁴ with virtually no alteration of the coordination geometry of the copper ion⁵ and of the catalytic properties of the enzyme⁶ ($\text{Cu}_2\text{Co}_2\text{SOD}$). This "innocent" substitution has, however, dramatic effects on the spectroscopic properties of the resulting derivative: magnetic

exchange coupling interactions between the high-spin cobalt(II) and the copper(II) centers take place, with an isotropic exchange coupling constant of 16.5 cm^{-1} (i.e., a separation of 33 cm^{-1} between the $S = 2$ and $S = 1$ multiplets, the latter being lower).⁷ This results in a dramatic shortening of the electronic relaxation times of copper(II) and therefore in the disappearance of its EPR spectrum. On the other hand, this allowed us to observe the ^1H NMR signals of the ring protons of the histidines coordinated to both the cobalt(II) and the copper(II) chromophores.⁵ Therefore, exchange coupling with cobalt(II) turns the copper(II) ion into a potentially precious NMR probe for the investigation of the system. For instance, it has been observed that upon addition of azide or cyanate, which are known to bind copper on the native protein,⁸⁻¹⁰ some of the isotropically shifted signals move toward

(1) Tainer, J. A.; Getzoff, E. D.; Beem, K. M.; Richardson, J. S.; Richardson, D. C. *J. Mol. Biol.* **1982**, *160*, 181-217.

(2) Fee, J. A. *J. Biol. Chem.* **1973**, *248*, 4229-4234.

(3) Calabrese, L.; Rotilio, G.; Mondovì, B. *Biochim. Biophys. Acta* **1972**, *263*, 827-829.

(4) Calabrese, L.; Cocco, D.; Morpurgo, L.; Mondovì, B.; Rotilio, G. *Eur. J. Biochem.* **1976**, *64*, 465-470.

(5) Bertini, I.; Lanini, G.; Luchinat, C.; Messori, L.; Monnanni, R.; Scozzafava, A. *J. Am. Chem. Soc.* **1985**, *107*, 4391-4396.

(6) Beem, K. M.; Rich, W. E.; Rajagopalan, K. V. *J. Biol. Chem.* **1974**, *249*, 7298-7305.

(7) Morgenstern-Badarau, I.; Cocco, D.; Desideri, A.; Rotilio, G.; Jordanov, J.; Dupre, N. *J. Am. Chem. Soc.* **1986**, *108*, 300-302.

(8) Rotilio, G.; Finazzi Agrò, A.; Calabrese, L.; Bossa, F.; Guerrieri, P.; Mondovì, B. *Biochemistry* **1971**, *10*, 616-621.

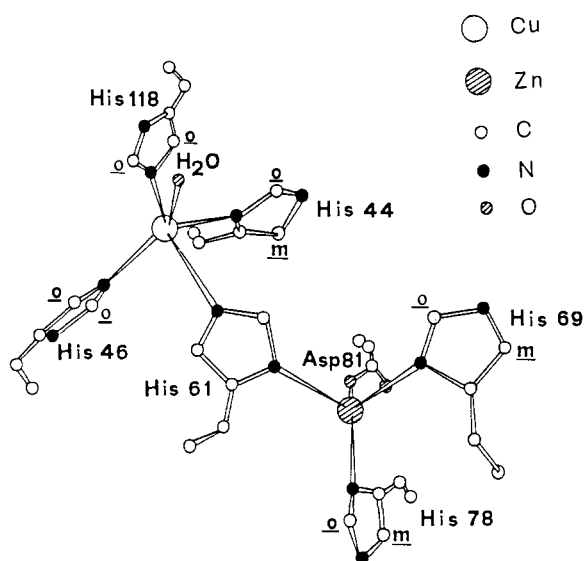
(9) Fee, J. A.; Gaber, B. P. *J. Biol. Chem.* **1972**, *247*, 60-65.

(10) Bertini, I.; Borghi, E.; Luchinat, C.; Scozzafava, A. *J. Am. Chem. Soc.* **1981**, *103*, 7779-7783.

Table I. Experimental and Calculated ^1H T_1 Values for $\text{Cu}_2\text{Co}_2\text{SOD}$ at 300 MHz and 300 K

| proton | $r_{\text{H-Cu}}$ (Å) | $r_{\text{H-Co}}$ (Å) | T_1 (ms) calcd with a single τ_s^a | T_1 (ms) calcd with two τ_s^b | T_1 (ms) calcd with two τ_s and L.C. contribution ^c | T_1 (ms) exptl | signal |
|------------------------|-----------------------|-----------------------|---|--------------------------------------|---|------------------|--------|
| His-61 H ϵ 1 | 3.29 | 3.26 | 0.17 | 0.44 | 1.08 | | |
| His-61 H δ 2 | 3.16 | 5.13 | 1.09 | 0.83 | 1.25 | 1.1 | A |
| His-44 H β 1 | 2.72 | 6.31 | 0.67 | 0.36 | 0.84 | 1.2 | P |
| His-78 H ϵ 1 | 7.61 | 3.08 | 0.13 | 0.50 | 1.27 | 1.4 | I |
| His-69 H ϵ 1 | 5.80 | 3.26 | 0.19 | 0.69 | 1.77 | 1.6 | J' |
| His-118 H ϵ 1 | 3.11 | 8.74 | 1.60 | 0.82 | 1.92 | 1.7 | H |
| His-44 H ϵ 1 | 3.28 | 5.79 | 1.63 | 1.08 | 2.53 | 2.4 | O |
| His-46 H δ 2 | 3.27 | 7.26 | 1.99 | 1.09 | 2.54 | 2.5 | M |
| His-118 H δ 2 | 3.27 | 8.05 | 2.11 | 1.11 | 2.59 | 2.5 | N |
| His-46 H ϵ 1 | 3.30 | 7.41 | 2.13 | 1.16 | 2.70 | 2.8 | G |
| His-78 H ϵ 2 | 9.90 | 4.89 | 2.11 | 7.92 | 2.98 | | F |
| His-78 H δ 2 | 10.57 | 5.03 | 2.50 | 0.39 | 3.05 | 3.1 | D |
| His-69 H ϵ 2 | 7.71 | 5.08 | 2.64 | 9.56 | 3.05 | | J |
| His-69 H δ 2 | 9.18 | 5.21 | 3.08 | 11.46 | 3.12 | 3.1 | E |
| His-118 H δ 1 | 4.91 | 10.35 | 22.37 | 12.55 | 4.23 | 4.1 | B |
| His-44 H δ 2 | 5.12 | 5.52 | 3.87 | 8.27 | 3.97 | 4.2 | L |
| His-44 H ϵ 2 | 5.09 | 5.65 | 4.33 | 8.64 | 4.00 | 4.5 | K |
| His-46 H δ 1 | 5.10 | 8.66 | 21.36 | 15.01 | 4.33 | | C |

^a $\tau_s = 2 \times 10^{-11}$ s. ^b $\tau_{s\text{Cu}} = 4 \times 10^{-11}$ s; $\tau_{s\text{Co}} = 5 \times 10^{-12}$ s. ^c $\tau_{s\text{Cu}} = 1.7 \times 10^{-11}$ s; $\tau_{s\text{Co}} = 1.2 \times 10^{-12}$ s; ligand-centered contribution (L.C.), $L = 4.3 \times 10^{44}$ cm⁻⁶.

**Figure 1.** Schematic drawing of the copper-zinc active site in superoxide dismutase.

the diamagnetic region of the spectrum. These signals were tentatively assigned as belonging to one of the nonbridging copper-coordinated histidines, suggesting that anions might remove a histidine from the coordination sphere. The aim of the present paper is to investigate the possibility of obtaining quantitative information on the structural changes accompanying anion binding. This has required a full understanding of the NMR parameters of the anion-free system. Advantage has been taken of some recent theoretical advances in the understanding of the NMR properties of exchange-coupled dimetallic systems.^{11,12}

Experimental Section

The $\text{Cu}_2\text{Co}_2\text{SOD}$ and $\text{E}_2\text{Co}_2\text{SOD}$ derivatives were prepared as described elsewhere.⁵ The $\text{Cu}_2\text{Co}_2\text{SOD}$ -azide derivative was obtained by making the solution 2×10^{-1} M in NaN_3 and 8.0×10^{-4} M in $\text{Cu}_2\text{Co}_2\text{SOD}$.

The ^1H NMR spectra were recorded on a Bruker WA 400, a Bruker CXP 300, a Varian XL 200, and a Bruker CXP 90, and, at 60 MHz, with a Bruker CXP console attached to a 1.4-T Varian electromagnet.

The spectra were recorded by using the modified DEFT pulse sequence^{13,14} in order to suppress H_2O (HDO) and bulk protein signals.

Typical spectra at 400, 300, and 200 MHz consisted of $\sim 10\,000$ scans with 16 000 data points over a 50 000-Hz bandwidth. Spectra at 90 and 60 MHz were obtained through block-averaging of 5–20 spectra of 16 000 scans each with 8000 data points over 50 000-Hz bandwidth. Chemical shifts were measured from the H_2O or HDO signals and reported from tetramethylsilane, assumed to be at -4.8 ppm from the water peak. Exponential multiplication of the free induction decay to improve the signal-to-noise ratio was such as to introduce a 20-Hz additional line broadening which was taken into account for line-width measurements.

The 300-MHz T_1 values of the $\text{Cu}_2\text{Co}_2\text{SOD}\cdot\text{N}_3^-$ derivative were determined by measuring the signals' intensity as a function of the time between subsequent pulses of the modified DEFT sequence.¹⁴

Results and Discussion

General Strategy. A full assignment of the isotropically shifted ^1H NMR signals in $\text{Cu}_2\text{Co}_2\text{SOD}$ is attempted by comparison of the metals-protons distances obtained from the X-ray structure with the T_1 values of these signals and the field dependence of their line widths. Such analysis is also expected to provide the correlation times for the unpaired electrons-nuclei interactions. These correlation times should then be used in the subsequent evaluation of the metal-nuclei distances in the N_3^- adduct. Hopefully, we should be able to pinpoint the protein residue which is most sensitive to azide binding and to describe its movement in the active site cavity.

Analysis of the T_1 Values. Figure 2 shows the 300-MHz ^1H NMR spectra of the $\text{Cu}_2\text{Co}_2\text{SOD}$ and of its azide derivative. Apart from the improved signal-to-noise ratio, the spectra are identical with those previously reported.⁵ As already noted,⁵ addition of azide ions to $\text{Cu}_2\text{Co}_2\text{SOD}$ solutions results in a progressive change of the resonance positions of the isotropically shifted signals; apparently, azide is in fast exchange on the time scale of the present NMR experiment, so that a one-to-one correspondence can be established between each signal in unligated $\text{Cu}_2\text{Co}_2\text{SOD}$ and in its azide adduct. Such correspondence is indicated by dashed lines in Figure 2.

Table I (7th and 8th columns) shows the 300-MHz T_1 values of the observed isotropically shifted signals in the $\text{Cu}_2\text{Co}_2\text{SOD}$ derivative.⁵ We take these values as the starting point for the assignment of the signals in $\text{Cu}_2\text{Co}_2\text{SOD}$ to the various protons of the residues coordinated to the two paramagnetic metal ions (Figure 1).

Theory for the nuclear magnetic resonance in paramagnetic systems predicts three different contributions to nuclear longitudinal relaxation by the unpaired electrons:¹⁵ one arises from

(11) Bertini, I.; Lanini, G.; Luchinat, C.; Mancini, M.; Spina, G. *J. Magn. Reson.* **1985**, *65*, 56–63.

(12) Owens, C.; Drago, R. S.; Bertini, I.; Luchinat, C.; Banci, L. *J. Am. Chem. Soc.* **1986**, *108*, 3298–3303.

(13) Bertini, I.; Gerber, M.; Lanini, G.; Luchinat, C.; Maret, W.; Rawer, S.; Zeppezauer, M. *J. Am. Chem. Soc.* **1984**, *106*, 1826–1830.

(14) Hochmann, J.; Kellerhals, H. P. *J. Magn. Reson.* **1980**, *38*, 23–29.

(15) Bertini, I.; Luchinat, C. *NMR of Paramagnetic Molecules in Biological Systems*; Benjamin Cummings: Menlo Park, CA, 1986.

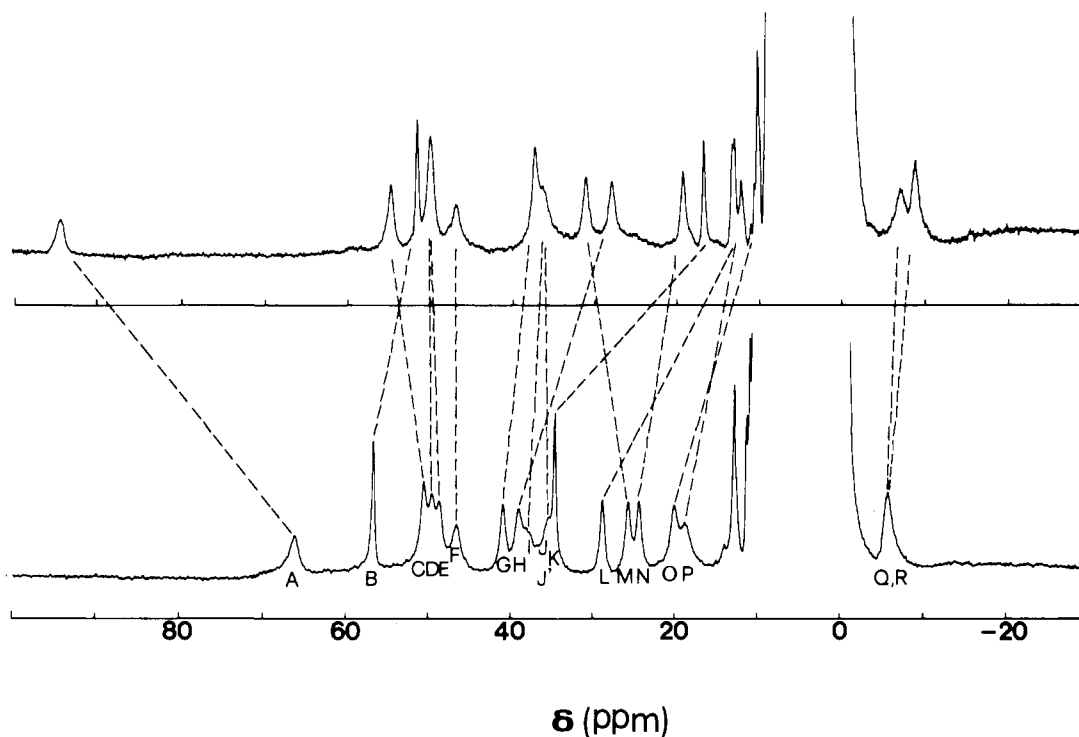


Figure 2. 300-MHz ^1H NMR spectra at 300 K and pH 5.6, acetate buffer, of: (A) $\text{Cu}_2\text{Co}_2\text{SOD}$ derivative; (B) $\text{Cu}_2\text{Co}_2\text{SOD} + \text{N}_3^- 2 \times 10^{-1} \text{ M}$.

through-space dipolar interaction between the unpaired spins residing on the metal and the observed nucleus; another contribution arises from a contact interaction between the nucleus and a fraction of unpaired spin directly delocalized, or induced by spin polarization, onto s orbitals of the nucleus itself; finally further dipolar contributions come from unpaired spin density residing on neighboring atoms. Although due to small fractions of the total spin, the two latter contributions may be sizable because the interaction is short-range (or even at "zero" distance in the case of contact coupling).

In the classic theory, the first two contributions are described by the well-known Solomon¹⁶–Bloembergen¹⁷ equations. The metal-centered dipolar term is given by:

$$T_{1M}^{-1} = \frac{2}{15} \gamma_1^2 g_e^2 \mu_B^2 r^{-6} S(S+1) \left(\frac{7\tau_s}{1 + \omega_s^2 \tau_s^2} + \frac{3\tau_s}{1 + \omega_1^2 \tau_s^2} \right) \quad (1)$$

while the contact term is:

$$T_{1M}^{-1} = \frac{2}{3} \left(\frac{A}{\hbar} \right)^2 S(S+1) \frac{\tau_s}{1 + \omega_s^2 \tau_s^2} \quad (2)$$

where γ_1 is the nuclear magnetogyric ratio of the nucleus, g_e is the electronic g factor, μ_B is the Bohr magneton, r is the electron–proton distance, ω_s and ω_1 are the electron and nucleus Larmor frequencies at the magnetic field of the experiment, τ_s is the electronic relaxation time, and A/\hbar is the Fermi contact coupling constant (in rad s^{-1}).

It has been recently shown that in exchange-coupled systems such equations should be modified to account for the different electronic situation described by a metallic pair with total spin S' .¹² This definitely holds when the energy separation between the $S' = 2$ and $S' = 1$ states is larger than the Zeeman energy as in the present case in which $|J| = 16.5 \text{ cm}^{-1}$. In such cases the contribution from each metal ion to the T_{1M}^{-1} of a particular proton is calculated to be proportional to the $S(S+1)$ value of the isolated ion times a reduction coefficient which, in a $S = 1/2/S = 3/2$ pair, is $3/8$ for the $S = 1/2$ ion and $7/8$ for the $S = 3/2$ ion¹² in the assumption that the $S' = 2$ and $S' = 1$ multiplets have the

same electronic relaxation times. Therefore, in $\text{Cu}_2\text{Co}_2\text{SOD}$, the metal-centered dipolar and contact contributions to the longitudinal relaxation rate of nucleus i are given by:

$$T_{1M}^{-1}(i) = \frac{2}{15} \gamma_1^2 g_e^2 \mu_B^2 \left[\frac{3}{8} S_{\text{Cu}}(S_{\text{Cu}} + 1) r_{i-\text{Cu}}^{-6} \times \left(\frac{7\tau_{s(\text{Cu})}}{1 + \omega_s^2 \tau_{s(\text{Cu})}^2} + \frac{3\tau_{s(\text{Cu})}}{1 + \omega_1^2 \tau_{s(\text{Cu})}^2} \right) + \frac{7}{8} S_{\text{Co}}(S_{\text{Co}} + 1) r_{i-\text{Co}}^{-6} \times \left(\frac{7\tau_{s(\text{Co})}}{1 + \omega_s^2 \tau_{s(\text{Co})}^2} + \frac{3\tau_{s(\text{Co})}}{1 + \omega_1^2 \tau_{s(\text{Co})}^2} \right) \right] + \frac{3}{8} \frac{2}{3} \left(\frac{A}{\hbar} \right)_{i-\text{Cu}}^2 S_{\text{Cu}}(S_{\text{Cu}} + 1) \frac{\tau_{s(\text{Cu})}}{1 + \omega_s^2 \tau_{s(\text{Cu})}^2} + \frac{7}{8} \frac{2}{3} \left(\frac{A}{\hbar} \right)_{i-\text{Co}}^2 S_{\text{Co}}(S_{\text{Co}} + 1) \frac{\tau_{s(\text{Co})}}{1 + \omega_s^2 \tau_{s(\text{Co})}^2} \quad (3)$$

It should be pointed out that in such an equation $\tau_{s(\text{Cu})}$ and $\tau_{s(\text{Co})}$ refer to the electronic relaxation times of the ions *in the pair*. These values are expected to be different from those of the isolated ions; in particular, the electronic relaxation time of the copper(II) ion will be much shortened by the interaction with the fast-relaxing cobalt(II) chromophore.

Since the $r_{i-\text{Cu}}$ and $r_{i-\text{Co}}$ values can be calculated with reasonable accuracy from the X-ray data (Table I, second and third columns), the unknowns in eq 3 are the τ_s values for the two ions plus the A/\hbar values for each nucleus with each metal ion. Our first task is therefore that of recalculating a set of T_1^{-1} values in the same ballpark of the experimental ones by using a reasonable choice for these parameters.

In a first step, the A/\hbar values were all taken equal to $4.8 \times 10^6 \text{ rad}^{-1}$ for the ring protons of the coordinated histidines. Such a value is an overestimate obtained from the McConnell equation¹⁸ and a default value of 100 ppm for the contact shift of all ring-proton signals. From this first set of calculations it clearly appeared that the contact term never contributes more than a few percent to the total T_{1M}^{-1} . This finding is independent of the choice of the τ_s values, since the latter are present in both the dipolar and contact terms. The relative contribution of the contact term

(16) Solomon, I. *Phys. Rev.* **1955**, *99*, 559–564.

(17) Bloembergen, N. *J. Chem. Phys.* **1957**, *27*, 572–573.

(18) McConnell, H. M.; Chesnut, D. B. *J. Chem. Phys.* **1958**, *28*, 107–117.

is, of course, even smaller if some ligand-centered effect is present (see below). Therefore, such a term has been left out of all subsequent calculations. Restricting ourselves to the metal-centered dipolar contribution, a first estimate of the two τ_s values was attempted.

By using values of $\tau_{s(\text{Cu})} = \tau_{s(\text{Co})} = 2 \times 10^{-11}$ s the set of the $T_{1\text{M}}^{-1}$ values in the fourth column of Table I were obtained. They range from 0.2 ms for ring protons in *ortho*-like positions with respect to the cobalt-coordinated nitrogen to 22 ms for ring protons in meta-like positions with respect to the copper-coordinated nitrogen. Clearly, this spread is much larger than that of the experimental values, no matter what the detailed assignment is. In particular, the T_1 values for cobalt ligands range from 0.13 to 3.08 ms, while those for the copper ligands range from 1.6 to 22 ms. Therefore, the two electronic relaxation times must differ to such an extent as to make the two subsets of calculated T_1 's more or less equal. A choice of $\tau_{s(\text{Cu})} = 4 \times 10^{-11}$ s and $\tau_{s(\text{Co})} = 5 \times 10^{-12}$ s gave the set of T_1 values shown in the fifth column of Table I. It appears that the spread is somewhat reduced, although the agreement is still far from being satisfactory. Already at this stage it can be stated, however, that (i) the electronic relaxation time of copper(II) has been dramatically reduced with respect to the isolated ion, but (ii) it is still sizably longer than that of the cobalt(II) ion.

Ligand-Centered Effects. The main discrepancy between the experimental and calculated T_1 's of column 5 is now in the large calculated difference between the T_1 's of the *ortho*- and *meta*-like protons. For a regularly coordinated imidazole moiety, the expected metal-centered dipolar contribution to the T_1^{-1} value of a metal-like proton is, in fact, smaller by a factor of 15–30 than that on an *ortho*-like proton, while all the experimental T_1 values range between 1 and 5 ms. To test whether this phenomenon was a peculiarity of the present system, we have performed ^1H NMR T_1 measurements on a series of cobalt(II) complexes (Figure 3); in histidine-containing systems the *meta*-/*ortho*-like T_1 ratios ranged between 2 and 4. Analogous ratios were previously observed in other cobalt(II)-substituted metallo proteins.^{13,19} We ascribe this behavior to the presence of sizable ligand-centered dipolar relaxation contributions on the imidazole ring protons. This seems to be a peculiarity of the histidine systems, since ligand-centered contributions are apparently much smaller in the six-membered ring of pyridine, and in the five-membered ring of *N*-methylimidazole (Figure 3).

In the absence of detailed knowledge of the spin density pattern on each histidine ring some assumptions have to be made. According to previous theoretical estimates of ligand centered effects on π systems, the observed ^1H T_1^{-1} values would be given by:

$$T_1^{-1} = T_{1\text{M}}^{-1} + T_{1\text{ML}}^{-1} + T_{1\text{L}}^{-1} \quad (4)$$

where $T_{1\text{L}}^{-1}$ is the contribution from the unpaired π spin density on the adjacent heteroatom (C or N), $T_{1\text{ML}}^{-1}$ is the cross term, and $T_{1\text{M}}^{-1}$ is a metal-centered effect due to the unpaired spin density on the metal orbitals.²⁰ MO calculations have shown that $T_{1\text{M}}^{-1}$ is sizably smaller than the theoretical point-dipole value for protons close to the paramagnetic center, i.e., partially within the metal electron cloud, and only approaches the point-dipole (Solomon) value for $r > 4 \text{ \AA}$.²¹ In the present system there are essentially two classes of aromatic protons; the first class is constituted by the *ortho*-like protons, with metal-proton distances in the 3.0–3.2- \AA range, and the second, by *meta*-like protons with distances in the 5.0–5.3- \AA range. It has been shown that, for protons at $\sim 3 \text{ \AA}$ from the metal, under the conditions of relatively strong π spin delocalization, the $T_{1\text{L}}^{-1}$ and $T_{1\text{ML}}^{-1}$ terms essentially compensate the decrease in the $T_{1\text{M}}^{-1}$ term with respect to the point dipole approximation, so that the total T_1^{-1} is accidentally close to the Solomon estimate.²¹ On the other hand, for *meta*-like

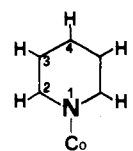
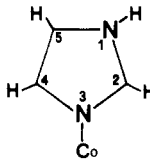
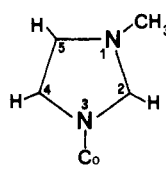
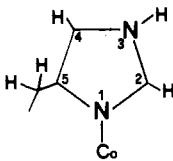
| SAMPLE | AROMATIC MOIETY | ^1H T_1 (ms) | | | |
|--------|--|-------------------------|-----|-----|-----|
| | | 2 | 3 | 4 | 5 |
| 1 |  | 7.5 | 140 | 270 | — |
| 2 |  | 1.5 | — | 2.4 | — |
| 3 |  | 2.9 | — | 2.9 | 4.3 |
| 4 |  | 2.9 | — | 5.0 | — |

Figure 3. T_1 values of ring protons of pyridine and imidazole moieties in high-spin cobalt(II) complexes at 90 MHz and 300 K. The data are obtained under the following conditions: sample (1) CoCl_2 1×10^{-4} M, pyridine 1×10^{-3} M, D_2O solvent; (2) $\text{Co}(\text{CH}_3\text{COO})_2(\text{imidazole})_2$ 1.4×10^{-1} M in CD_3OD ; (3) cobalt(II) acetate 1.1×10^{-1} M, 1-methylimidazole 5.5×10^{-1} M, CD_3OD solvent; (4) cobalt(II) acetate 2×10^{-1} M, histidine 4×10^{-1} M, D_2O solvent.

protons, the total T_1^{-1} is essentially equal to the Solomon estimate plus a sizable contribution given by $T_{1\text{ML}}^{-1} + T_{1\text{M}}^{-1}$. The latter is expected to be dominant. Therefore, we have chosen to use the Solomon equation as such for the *ortho*-like protons, and to substitute $1/r^6$ with a term $1/r^6 + L$ for *meta*-like protons, L being an adjustable parameter accounting for $T_{1\text{ML}}^{-1} + T_{1\text{L}}^{-1}$ contributions and equal for all *meta*-like protons of the system.

Together with the two τ_s values, this gives a total of three unknowns for as many equations (14) as the total number of T_1 values available for isotropically shifted signals. Column 6 of Table I shows the results obtained with $\tau_{s(\text{Cu})} = 1.7 \times 10^{-11}$, $\tau_{s(\text{Co})} = 1.2 \times 10^{-12}$ s, and an L value of $4.3 \times 10^{44} \text{ cm}^{-6}$; the range of values is now in excellent agreement with the experimental one (for the detailed assignment, see later).

Analysis of the Field Dependence of the Line Width. Table II shows the T_2 values of the isotropically shifted signals in $\text{Cu}_2\text{-Co}_2\text{SOD}$ at 60, 90, 200, 300, and 400 MHz obtained from the relation $T_2 = (\pi\Delta\nu)^{-1}$, where $\Delta\nu$ is the line width at half-peak height. The $\Delta\nu$ values have been obtained through computer-simulation of the experimental spectra using Lorentzian line shape for all the signals. Computer simulation is far superior to direct half-height line-width measurements when complex envelopes of signals are present. The estimated indeterminations of all the values reported in Table II is always smaller than $\pm 20\%$, except for signal J' which is not apparent from the spectrum.

Theory predicts that the paramagnetic effects operative on T_2 values are analogous to those determining T_1 ,¹⁵ i.e., metal- and ligand-centered dipolar and contact mechanisms, plus a contribution arising from the time-averaged magnetic moment of the system, modulated by the rotational time of the molecule.^{22,23} The

(19) Bertini, I.; Canti, G.; Luchinat, C.; Mani, F. *J. Am. Chem. Soc.* **1981**, *103*, 7784–7788.

(20) Doddrell, D. M.; Healy, P. C.; Bendall, M. R. *J. Magn. Reson.* **1978**, *29*, 163–168.

(21) Gottlieb, H. P. W.; Barfield, M.; Doddrell, D. M. *J. Chem. Phys.* **1977**, *67*, 3785–3789.

Table II. Line Widths (Hz) at 300 K for the ^1H Signals of $\text{Cu}_2\text{Co}_2\text{SOD}$ at Various Magnetic Fields

| signal | 60 MHz | | 90 MHz | | 200 MHz | | 300 MHz | | 400 MHz | |
|--------|--------|-------|--------|-------|---------|-------|---------|-------|---------|-------|
| | exptl | calcd | exptl | calcd | exptl | calcd | exptl | calcd | exptl | calcd |
| A | 230 | 393 | 220 | 385 | 360 | 428 | 440 | 544 | 512 | 728 |
| B | 115 | 97 | 110 | 92 | 130 | 93 | 115 | 98 | 124 | 106 |
| C | 150 | 95 | 120 | 90 | 170 | 91 | 230 | 96 | 310 | 104 |
| D | 180 | 202 | 170 | 203 | 200 | 245 | 295 | 353 | 395 | 525 |
| E | 120 | 197 | 170 | 198 | 195 | 239 | 295 | 345 | 395 | 513 |
| F | 200 | 207 | 190 | 208 | 270 | 251 | 460 | 361 | 540 | 538 |
| G | 130 | 152 | 130 | 145 | 160 | 146 | 240 | 155 | 284 | 169 |
| H | 220 | 213 | 260 | 204 | 240 | 205 | 320 | 216 | 360 | 233 |
| I | 380 | 484 | 290 | 487 | 395 | 588 | 520 | 846 | 630 | 1258 |
| J' | 480 | 346 | 280 | 348 | 410 | 418 | 550 | 600 | 930 | 892 |
| J | 280 | 201 | 160 | 202 | 275 | 244 | 350 | 351 | 474 | 522 |
| K | 160 | 106 | 80 | 102 | 80 | 105 | 95 | 116 | 117 | 135 |
| L | 190 | 108 | 106 | 104 | 160 | 107 | 200 | 120 | 255 | 140 |
| M | 160 | 162 | 115 | 155 | 210 | 156 | 240 | 166 | 280 | 181 |
| N | 160 | 158 | 120 | 151 | 205 | 152 | 235 | 161 | 280 | 175 |
| O | 250 | 165 | 190 | 158 | 250 | 161 | 280 | 175 | 340 | 196 |
| P | 330 | 488 | 250 | 467 | 340 | 470 | 480 | 498 | 530 | 540 |

size of the latter contribution, termed Curie-spin relaxation, increases with the square of the magnetic field. If the analysis performed on the T_1 values is correct, the same kind of analysis, with the addition of the Curie-spin term, should be able to reproduce also the experimental T_2 patterns.

The equation used to reproduce the values in Table II has the following form:

$$T_{2M}^{-1}(i) = \frac{1}{15} \gamma_1^2 g_e^2 \mu_B^2 \left[\frac{3}{8} S_{\text{Cu}}(S_{\text{Cu}} + 1) r_{i-\text{Cu}}^{-6} \left(\frac{13\tau_{s(\text{Cu})}}{1 + \omega_s^2 \tau_{s(\text{Cu})}^2} + \frac{3\tau_{s(\text{Cu})}}{1 + \omega_1^2 \tau_{s(\text{Cu})}^2} + 4\tau_{s(\text{Cu})} \right) + \frac{7}{8} S_{\text{Co}}(S_{\text{Co}} + 1) r_{i-\text{Co}}^{-6} \times \left(\frac{13\tau_{s(\text{Co})}}{1 + \omega_s^2 \tau_{s(\text{Co})}^2} + \frac{3\tau_{s(\text{Co})}}{1 + \omega_1^2 \tau_{s(\text{Co})}^2} + 4\tau_{s(\text{Co})} \right) \right] + \frac{3}{8} \frac{1}{3} \left(\frac{A}{\hbar} \right)_{i-\text{Cu}}^2 S_{\text{Cu}}(S_{\text{Cu}} + 1) \left(\tau_{s(\text{Cu})} + \frac{\tau_{s(\text{Cu})}}{1 + \omega_s^2 \tau_{s(\text{Cu})}^2} \right) + \frac{7}{8} \frac{1}{3} \left(\frac{A}{\hbar} \right)_{i-\text{Co}}^2 S_{\text{Co}}(S_{\text{Co}} + 1) \left(\tau_{s(\text{Co})} + \frac{\tau_{s(\text{Co})}}{1 + \omega_s^2 \tau_{s(\text{Co})}^2} \right) + \frac{1}{5} \frac{\omega_1^2 g_e^4 \mu_B^4 S_{\text{Cu}}^2 (S_{\text{Cu}} + 1)^2}{(3\kappa T)^2 r_{i-\text{Cu}}^6} \left(4\tau_r + \frac{3\tau_r}{1 + \omega_1^2 \tau_r^2} \right) + \frac{1}{5} \frac{\omega_1^2 g_e^4 \mu_B^4 S_{\text{Co}}^2 (S_{\text{Co}} + 1)^2}{(3\kappa T)^2 r_{i-\text{Co}}^6} \left(4\tau_r + \frac{3\tau_r}{1 + \omega_1^2 \tau_r^2} \right) \quad (5)$$

where the last two terms represent the Curie-spin contributions from the two metal ions and all the others are analogous to the corresponding terms in eq 3. Before discussing the results of the line-width analysis, a few comments are appropriate on the form of eq 5. (i) We have chosen to use the 3/8 and 7/8 coefficients in all the terms corresponding to those in eq 3, i.e., metal- and ligand-centered dipolar contributions, although the theoretical frame in which these coefficients were calculated referred only to T_1 values. However, the physics underlying T_1 and T_2 relaxation phenomena is the same, and there is no reason to expect the exchange coupling between two paramagnetic centers should not influence T_2 as well. (ii) Ligand-centered effects have been introduced in the Curie-spin relaxation term, i.e., by substituting $1/\tau^6$ with a term $1/\tau^6 + L$ for meta-like protons; to our knowledge, this is the first time that such effects are taken into account in the analysis of the field-dependent line broadening originated by

Table III. 300-MHz Experimental and Calculated ^1H T_1 and $(\pi T_2)^{-1}$ Values for the Meta-like Protons in $\text{E}_2\text{Co}_2\text{SOD}$ Derivative at 300 K^a

| proton | T_1 (ms) | | $(\pi T_2)^{-1}$ (Hz) | | signal (shift in ppm) |
|-----------------------|------------|-------|-----------------------|-------|--------------------------|
| | exptl | calcd | exptl | calcd | |
| His-69 H δ 2 | 1.2 | 1.29 | 340 | 302 | 54.9 |
| His-61 H δ 2 | 1.4 | 1.34 | 430 | 327 | 50.9 |
| His-69 H ϵ 2 | 1.4 | 1.35 | 370 | 311 | 47.7 |
| His-78 H ϵ 2 | 1.3 | 1.33 | 430 | 327 | 44.5 |

^a Because of the similarity of the calculated T_1 and T_2 values, a correlation between experimental and calculated values cannot be established.

Curie-spin, but, again, there is no physical reason to neglect the coupling with the time-averaged magnetic moment delocalized onto ligand nuclei. (iii) The reduction coefficients 3/8 and 7/8 have *not* been included into the Curie-spin term. This choice is due to the fact that Curie-spin relaxation depends on the square of $\langle S_z \rangle$, i.e., is proportional to the static magnetic susceptibility of the system. For a J value of 16.5 cm^{-1} the magnetic susceptibility of the Cu-Co pair at room temperature is just the sum of the susceptibilities of the isolated ions; this has also been experimentally verified on the present system.⁵ Therefore, the two metal centers should be considered as uncoupled as far as Curie-spin relaxation is concerned.

In order to test the validity of the T_1^{-1} analysis, the same values for the three parameters (i.e., $\tau_{s(\text{Cu})}$, $\tau_{s(\text{Co})}$, and L) have been used also in eq 5. This leaves only the rotational correlation time, τ_r , as adjustable parameter to reproduce the experimental T_2 values for 17 signals at five magnetic field values. A good agreement is obtained for a τ_r value of 5×10^{-9} s, and the results are shown in Table II. It appears that all the values, except those of signal C, are reproduced within a factor of 2. This is a remarkable result if it is considered that it has been achieved with only one adjustable parameter, which also compares very well with the estimate of 4×10^{-9} s from the Stokes-Einstein equation by taking the rotational radius equal to 16.5 \AA . Moreover, all the features of the field dependence are reproduced, like the initial increase in T_2 with magnetic field (between 60 and 90 MHz) and the sizable difference in the importance of the Curie-spin term for the protons of histidines coordinated to cobalt(II) with respect to those of histidines coordinated to copper(II). Possible reasons for discrepancy between calculated and experimental T_2^{-1} values are (i) the use of a single L value for all the meta-like protons (which is expected to give analogous discrepancies on T_1); (ii) the use of a single τ_r for the nonspheric molecule; (iii) possible chemical exchange between different equilibrium positions due to librations or proton exchange.

The $\text{E}_2\text{Co}_2\text{SOD}$ Derivative. Although not strictly relevant to the present analysis, a comment is due to the T_1 and T_2 data of the copper-depleted superoxide dismutase derivative in which

(22) Gueron, M. *J. Magn. Reson.* **1975**, *19*, 58-63.(23) Vega, A. J.; Fiat, D. *Mol. Phys.* **1976**, *31*, 347-355.

zinc(II) is substituted by cobalt(II). The NMR signals of this derivative are easily assigned to the ring protons of His-61, -69, and -78. The 300-MHz T_1 values of the signals of the meta-like protons (Table III) are sizably shorter than most of those of $\text{Cu}_2\text{Co}_2\text{SOD}$. An isolated cobalt(II) ion is, in fact, expected to experience a somewhat longer τ_s value. The data can be analyzed as described before, by using the same L value and the appropriate crystallographic distances. Table III shows the calculated values obtained with a τ_s value of 4×10^{-12} s. Such a value is longer than that observed in the coupled system. Apparently, in the coupled system, additional electronic relaxation mechanisms are operative also for the fast relaxing ion.

By using the above L and τ_s values, the 300-MHz T_2 data for the meta-like protons can be reproduced with the same τ_r value used for the $\text{Cu}_2\text{Co}_2\text{SOD}$ derivative, thus further confirming the overall validity of the approach.

A comment is due to the value of τ_s (4×10^{-12} s) obtained for the $\text{E}_2\text{Co}_2\text{SOD}$ derivative. Such a value is shorter than expected for a pseudotetrahedral cobalt(II) chromophore ($\sim 10^{-11}$ s). It has been shown, however, that if the zero-field splitting of the ion is taken into account when analyzing nuclear relaxation data,²⁴ values larger by about a factor of 3 are obtained with respect to the Solomon treatment as used in the present analysis. This would bring τ_s to a more plausible value of 10^{-11} s.

Evaluation of the Proposed Assignment. The analysis of the T_1 and T_2 values together allows us to discriminate between protons of cobalt ligands and protons of copper ligands, and to define four groups of protons. One is with T_1 values ranging from 4.1 to 4.5 ms, which are assigned to meta-like protons of copper-coordinated histidines. A second group of two signals with T_1 of 3.1 ms is assigned to meta-like protons of histidines bound to cobalt(II). A third group of five signals with T_1 ranging from 1.7 to 2.8 ms is assigned to protons in ortho-like positions of copper-coordinated histidines. Signal H has an exceptionally short T_1 value on account of its short proton-copper distance. However, its T_2 value confirms the assignment to a copper-ligand proton. The final set contains four signals, with T_1 's ranging from 1.1 to 1.6 ms. Two of these (i.e., I and J') are assigned to ortho-like protons of histidines bound to cobalt(II), and the signal with shortest T_1 (i.e., 1.1 ms) is assigned to the H δ 2 of His-61 which is meta to cobalt and ortho to copper. The signal with T_1 of 1.2 ms is assigned to one of the β -CH₂ protons of His-44, which is at a very short distance from copper, on a chemical basis (see later); the T_2 values are consistent with this assignment. From the present assignment we find that a proton of the bridging histidine, ortho to cobalt and ortho to copper, is missing, probably because it has escaped detection. A further step in the assignment is advanced by assigning the NH signals in the meta-like protons groups. The analysis of the azide derivative suggests that: signals L (meta-like), K (NH), O (ortho-like) and P (β -CH) belong to the same residue, i.e., His-44, which is the only copper-coordinated residue having a meta-like proton and a β -CH₂ proton very close to the copper ion.

Analysis of the $\text{Cu}_2\text{Co}_2\text{SOD}\cdot\text{N}_3^-$ Derivative. The above analysis allows us to attempt a detailed description of the $\text{Cu}_2\text{Co}_2\text{SOD}\cdot\text{N}_3^-$ system. Addition of azide causes the isotropic shift of signals K, L, O, and P to definitely go toward the diamagnetic region. We have already proposed that azide displaces one histidine residue from coordination to copper(II). This histidine is not the bridging one because the Co-Cu coupling is fully maintained as witnessed by the observation of all the proton signals from the copper(II) chromophore in the adduct. We had tentatively indicated His-44 as a possible candidate.⁵ Indeed, the present assignment confirms that one of the signals which are shifted toward the diamagnetic region of the spectrum upon azide binding (signal L) can be unequivocally assigned to the H δ 2 signal of His-44. The assignment of signal O to His-44 H ϵ 1 is also in agreement with the titration behavior. The T_1 values of these signals, as well as their T_2 values, are sizably increased, indicating a sizable reduction of

Table IV. ^1H T_1 Values and Estimated Cu-H Distances for the N_3^- Adduct of $\text{Cu}_2\text{Co}_2\text{SOD}$ ^a

| His-44 protons | $\text{Cu}_2\text{Co}_2\text{SOD} + \text{N}_3^-$ | | $\text{Cu}_2\text{Co}_2\text{SOD}$ | |
|--------------------------|---|-----------------------|------------------------------------|------------------|
| | T_1 (ms) exptl | $r_{\text{Cu-H}}$ (Å) | $r_{\text{Cu-H}}$ (Å) | T_1 (ms) exptl |
| <i>o</i> -H | 2.8 | 3.36 | 3.28 | 2.4 |
| N-H | 19.1 | 4.95 | 5.09 | 4.5 |
| <i>m</i> -H | 10.9 | 4.36 | 5.12 | 4.2 |
| β -CH ₂ | 8.7 | 3.68 | 2.72 | 1.2 |

^a For comparison purposes the experimental distances and T_1 values for the native enzyme are reported.

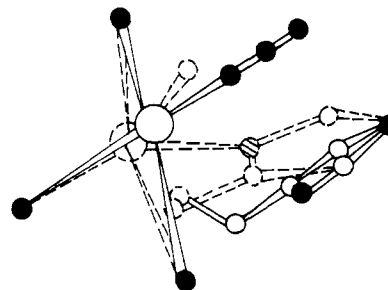


Figure 4. Sketch of the new arrangement of the histidines' nitrogens and of His-44 when the azide anion is bound to copper. The dashed lines are relative to native protein structure.

the experienced paramagnetic effect. Such reduction can be produced by an increase of the copper-proton distances, and/or by a drastic decrease in the ligand-centered contributions.

The present experimental data can thus be used to map the new position of the His-44 residue with respect to the copper ion in the azide derivative. Examination of the 300-MHz T_1 and T_2 values of the other signals in the azide adduct shows that very little changes have occurred in these parameters upon azide binding. Therefore, the same $\tau_{s(\text{Cu})}$ and $\tau_{s(\text{Co})}$ values can be confidently used for this derivative in order to calculate new r values. The L values have been set to zero for such protons since the isotropic shifts of the protons of His-44 tend to zero.

The calculated r values are shown in Table IV. It is immediately evident that the changes with respect to the crystallographic data are rather small, and some distances are even shorter than those in the unligated derivative. However, the position of the metal ion with respect to the three ring protons, which can be unequivocally determined by triangulation, has changed in a significant way, as shown in Figure 4. Indeed the metal ion is clearly *not* coordinated to the N1 nitrogen any longer, consistently with the isotropic shift data. This position qualitatively accounts for the residual isotropic shift which would be dipolar in origin in this frame. It is apparent from Figure 4 that a rotation of the His ring around the C_β - C_γ axis by about 60° together with a movement of the copper ion toward the plane formed by the N ϵ 2 nitrogens of His-46, -61, and -118, qualitatively accounts for the new copper-proton distances.

These results also justify the a priori choice of $L = 0$, which anticipated a noncoordinated histidine ring. If L were given nonzero value, all the calculated Cu-meta-H distances would be sizably longer. This would contradict the choice of $L \neq 0$, since sizable unpaired spin density cannot be present in a noncoordinated residue.

Inspection of the X-ray coordinates of nearby residues shows that such movement of His-44 is allowed although, of course, smaller adjustments may be propagated in its neighborhood. In particular, the hydrogen bond between N ϵ 2 and Asp-122 can be easily maintained. The lengthening of the Cu- β CH₂ distance can be partly accounted for by the upward movement of the copper(II) ion with respect to the original Cu-N ϵ 4 plane. Such movement is in perfect agreement with the picture of azide occupying the "water binding site" described by Tainer et al.²⁵ and with the axialization of the EPR spectrum of native SOD upon azide

(24) Bertini, I.; Luchinat, C.; Mancini, M.; Spina, G. *J. Magn. Reson.* **1984**, *59*, 213-222.

(25) Tainer, J. A.; Getzoff, E. D.; Richardson, J. S.; Richardson, D. C. *Nature (London)* **1983**, *306*, 284-287.

binding. The equatorial plane of copper in the adduct, defined by the N ϵ 2 nitrogens of His-61, -46, and -118 and by an azide nitrogen, would thus be tilted by about 30–40° with respect to the original plane.

Conclusions

The factorization into metal-centered and ligand-centered nuclear relaxation contributions has allowed us to account for the experimental T_1 values, especially for the ratio between ortho-like and meta-like proton T_1 's. By relating metal-centered contributions and proton-metal distances with appropriate equations, most of the signals have been unequivocally assigned to specific protons. The last ambiguities have been resolved by analysis of Curie contribution to line width which is also related to metal-proton distances.

The copper-cobalt magnetic coupling ($J = 16.5 \text{ cm}^{-1}$)⁷ causes a decrease in the electronic relaxation times of copper by a factor of 10^2 and that of cobalt by a factor of 3.²⁶ It might have been qualitatively predicted that magnetic coupling would have caused a decrease in τ_{s1} of the slow relaxing ion (copper), but the relation, if any, between J/\hbar and such a decrease, is unknown. When J/\hbar is smaller than τ_{s1}^{-1} (slow relaxing ion), the above effect can be expected to be negligible.^{12,27} When J/\hbar is intermediate between τ_{s1}^{-1} and τ_{s2}^{-1} (fast relaxing ion, i.e., cobalt) but close to the former, a relationship is proposed on a perturbative basis.¹¹ Nothing is known when J/\hbar is of the order of magnitude of τ_{s2}^{-1} except that the Solomon equation should be multiplied by a coefficient.¹² Again, qualitatively, when J/\hbar is much larger than τ_{s2}^{-1} , then both ions should experience the same τ_s^{-1} equal to the sum of τ_{s1}^{-1} and τ_{s2}^{-1} .

This holds if the magnetically coupled system does not provide independent and efficient relaxation pathways.

In the present case, J is such that the separation between $S' = 2$ and $S' = 1$ states is three times $\hbar\tau_{s2}^{-1}$ and the two τ_s still are different. It is possible that the nature of the mechanisms giving rise to magnetic coupling, i.e., exchange or superexchange,

(26) Associated Editor Sunney I. Chan suggested that the multiplets arising from magnetic coupling, $S'_1 = 1$ and $S'_2 = 2$, may have different electronic relaxation times. Of course, this may be true, and the system may even be more complicated by including zero-field splitting of the cobalt(II) ion²⁴ as well as of the $S'_1 = 1$ and $S'_2 = 2$ terms. If we consider that the two (zero-field unsplit) $S'_1 = 1$ and $S'_2 = 2$ levels have strongly different τ_s values, then essentially only one will contribute to nuclear relaxation (i.e., the multiplet with longer τ_s), and therefore the coefficients in eq 3 and in the first terms of eq 5 are calculated to be smaller than 3/8 and 7/8 (see below), and longer τ_s values for the two metal ions are predicted. If the $S'_1 = 1$ multiplet is dominating nuclear relaxation, the coefficients decrease by up to a factor of 6 and the new τ_s values are: $\tau_{s(\text{Cu})} = 1.1 \times 10^{-10}$ s and $\tau_{s(\text{Co})} = 5.5 \times 10^{-12}$ s. There are no consequences on the reproduction of the T_1 and T_2 values and on structural information. In the case where the $S'_2 = 2$ manifold has larger τ_s , the coefficients decrease by up to 40%, with smaller changes in τ_s values ($\tau_{s(\text{Cu})} = 2.0 \times 10^{-11}$ s, $\tau_{s(\text{Co})} = 2.7 \times 10^{-12}$ s) and with no consequence on the above discussion. These considerations show that in any case the τ_s of copper is much shorter than that in the uncoupled system, although still much longer than that of cobalt(II).

(27) Bertini, I.; Luchinat, C.; Owens, C.; Drago, R. S., paper in preparation.

is also important. In the present case a large superexchange contribution is proposed.²⁸

The detailed assignment of each proton which resulted for this present study and the knowledge of the correlation times makes NMR spectroscopy a powerful tool to monitor structural changes upon perturbing the system. For example, by adding N_3^- to the solution, the NMR parameters of all but four signals remain essentially unchanged; four signals move toward the diamagnetic position. They are the three ring protons of His-44 and that proton of $\beta\text{-CH}_2$ of the same residue which is found by X-ray very close to copper. The T_1 values of such signals indicate a movement of this histidine as shown in Figure 4.

Acknowledgment. The following laboratories are acknowledged for allowing us to record the ^1H NMR spectra at various magnetic fields: the Department of Chemistry, University of Siena, for the 200-MHz spectra; the high-field NMR Service Center, CNR, Bologna, for the 300-MHz spectra; Spectrospin A.G., Zürich, for the 400-MHz spectra. R. Pierattelli is acknowledged for performing some of the computer simulations of the spectra in order to obtain reliable line widths. The discussions with the friends of the Physics Department, M. Mancini and G. Spina, are also warmly acknowledged. Finally, we are grateful to D. Richardson (Duke University, Durham, NC) for extensive discussion of the likelihood of the proposed movement of His-44 within the active site cavity. This work has been performed with the contribution of the Progetto Strategico Biotecnologie del CNR.

Appendix

Calculation of the Coefficients for $S' = 1$ and $S' = 2$ Multiplets

The 3/8 and 7/8 coefficients (X) for copper(II) and cobalt(II) are obtained from:¹²

$$X_{\text{Cu}} = \frac{1}{S_{\text{Cu}}(S_{\text{Cu}} + 1)} \sum_i \left(C_{\text{Cu},i}^2 S'_i (S'_i + 1) \frac{2S'_i + 1}{\sum_i (2S'_i + 1)} \right)$$

$$X_{\text{Co}} = \frac{1}{S_{\text{Co}}(S_{\text{Co}} + 1)} \sum_i \left(C_{\text{Co},i}^2 S'_i (S'_i + 1) \frac{2S'_i + 1}{\sum_i (2S'_i + 1)} \right)$$

where $S_{\text{Cu}} = 1/2$, $S_{\text{Co}} = 3/2$, $S'_1 = 1$, $S'_2 = 2$, and $C_{\text{Cu},i}$ and $C_{\text{Co},i}$ are the standard spin-Hamiltonian coefficients for exchange-coupled systems.^{12,29}

By taking only the first ($S' = 1$ dominant) or the second ($S' = 2$ dominant) term in the summation, the X coefficients become

$$X_{\text{Cu}} = 1/16; X_{\text{Co}} = 5/16 \quad (S' = 1 \text{ dominant})$$

$$X_{\text{Cu}} = 5/16; X_{\text{Co}} = 9/16 \quad (S' = 2 \text{ dominant})$$

Registry No. SOD, 9054-89-1; His, 71-00-1; N_3^- , 14343-69-2.

(28) Bencini, A.; Gatteschi, D.; Zanchini, C.; Haasnoot, J. G.; Prins, R.; Reedijk, J. *Inorg. Chem.* **1985**, *24*, 2812–2817.

(29) Gatteschi, D. In *The Coordination Chemistry of Metalloenzymes*; Bertini, I., Drago, R. S., Luchinat, C., Eds.; D. Reidel Publishing Co.: Dordrecht, 1983; p 215.